Appendix VIII-A

Techniques Used to Compute the Output of Representative Collector Designs

The major variables which must be *con*sidered in analyzing collector performance were reviewed in a qualitative way in the main body of this chapter. This appendix indicates how these effects can be quantified and shows how the equations are derived which were used to obtain the detailed estimates of collector performance presented elsewhere in this report. Following the taxonomy of effects used in the earlier discussion, this presentation begins with a discussion of techniques for deriving estimates of the intensity of direct and indirect sunlight which can be captured by each collector geometry. It then provides a detailed discussion of the optical and thermal losses experienced by each major collector type.

AVAILABLE SUNLIGHT

Sunlight Data

As noted earlier, data about available sunlight around the country is of extremely uneven quality. Very few stations have measured direct normal sunlight, and results of these measurements have not been readily available. **Information** on the total amount of solar energy reaching a horizontal **surface is available from about 80** locations around the country and is archived in the National Climatic Center in Asheville, N.C. While this data does not distinguish between direct normal radiation and diffuse radiation, statistical techniques have been developed which can be used to approximate the relative contributions of the two types of radiation. The technique used in this study is based on work completed recently by Sandia Laboratories.

The basis for the Sandia analysis is the observation that the intensity of direct normal radiation is correlated with the ratio between the amount of energy actually reaching a horizontal surface in a given hour and the amount of energy which would have fallen on the surface if the Earth had no atmosphere. This ratio is called the "percent possible" sunshine and will be represented by the variable PP. The Sandia work compared the intensity of direct normal radiation (I_{DN}) as a function of PP in several locations where measurements of I_{DN} were available. It was found that the relationship could be approximated with a simple segmented straight-line formula which takes the following form:

$$_{DN} = \begin{cases} 0 & \text{when PP is less than or equal to 0.3} \\ A \cdot PP + B & \text{when PP is greater than 0.3 but less than or equal to C} \\ M & \text{when PP is greater than C} \end{cases} \tag{A-1}$$

where *A, B, C,* **and M are constants which must be determined for each location.** The values of these constants which apply to the three cities (for which consistent direct normal sunlight data is available) are shown in table **VII I-A-I.** Notice that in Albuquerque it was necessary to use different constants for midday and periods early and late in the day. In the analysis of sunlight data for Fort Worth, average values of the constants were used (A = 1.79, B = –0.55, C =0.85, and M = 1.00).

The data actually used for the estimates of collector performance conducted as a part of this study was taken at weather stations during 1962 (1963 in Boston). Table VII I-A-2 compares the average values of direct normal, and total horizontal radiation measured **at** these stations (and reduced us-

[1] **E** ldon C Bees, *Estimating the Direct Component of Solar Radiation,* Sandia Laboratories Energy Report, SAND 75-0565, November 1975

Table VIII-A-1 .—Empirically Derived Constants Used in the Formula for Estimating Direct Normal Radiation, Given Measurements of Total Horizontal Radiation (see equation A-l)

	Spring		Summer		Fall		Winter	
	Albuquerque*							
	Mid	E-L	*Mid*	*E-L*	*Mid*	*E-L*	*Mid*	*E-L*
A	1.64	1.13	1.65	1.07	1.56	1.15	2.42	1.68
B	-0.43	-0.19	-0.35	-0.17	-0.47	-0.21	-0.78	-0.25
C	0.85	0.85	0.80	0.80	0.85	0.85	0.80	0.80
M	1.07	1.07	0.95	0.95	0.97	0.97	1.09	1.09
	Blue Hill							
A	1.60		1.86		1.93		2.10	
B	-0.52		-0.56		-0.58		-0.71	
c	0.80		0.70		0.75		0.80	
M	0.89		0.81		0.87		1.03	
	Omaha							
A	1.69		1.62		1.88		1.67	
B	-0.62		-0.50		-0.68		-0.48	
c	0.85		0.80		0.85		0.85	
M	0.89		0.87		0.96		0.98	

"In Albuquerque, It was necessary to have separate Sets of constants for mldday (Mld)andearlyand late ln the day (E-L)

SOURCE Bees, Eldon, "Estimating the Direct Component of Solar Radiation," Sandia Laboratories Energy Report, SAND 75-0565, November 1975

ing the methods previously discussed) with average values of these quantities for a 15-year period. The 15-year averages were computed from data prepared by the National Climatic Center and the Aerospace Corporation. The 15-year average values shown **in the table contain correction factors which compensate** for calibration errors recently discovered in some of the older measuring equipment. While, as expected, the 1962 data does not precisely match the long-term average, no systematic error is apparent—some of the 1962 averages are higher while others are lower than the 15-year averages. Since observing sites a few miles apart can take measurements of sunlight and temperature which differ by 10 percent during the same year (because of microclimates producing local patterns of fog, etc.), the *1962* data probably represent a reasonable estimate of insolation as it is reasonable to make, given other errors inherent in projecting the cost of solar energy.

Direct Normal Radiation

The amount of direct normal radiation incident on a collector which is not directly facing the Sun is reduced by a factor equal

Table Vlll-A-2.—Comparison of 1962* Weather With Long-Term Averages and Extremes

Average daily sunlight ($kWh/m^2/day$)	Albuquerque	Boston	Fort Worth	Omaha
Direct normal 1962.	**7.0**	**3.9**	**4.3**	**4.0**
15+ yr av •. . . . .**	**7.1**	**3.3**	**4.7**	**4.5**
Ratio: average/1962.	1.01	**0.85**	**1.09**	**1.13**
Total on horizontal surface, 1962 . . .	5.5	3.7	4.5	4.2
15 + yr av . . . .**	5.8	3.5	4.7	4.2
Ratio: average/1962.	**1.05**	**0.95**	**1.04**	**1.00**
Heating degree-days† 1962	4,310	5,754	2,434	6,272
1954-74 average	4,374	5,769	2,423	6,145
1954-74 extremes.	3,857-4,941	5,410-6,228	1,861-2,855	5,622-6,911

"Read as 1963 for Boston wherever 1962 is used

“” 15 + year average was compiled from the augmented SOLMET weather tapes produced by the National Cllmatlc Center and the Aerospace Corporation.

†Heatlng degree-day information from "Local Cllmatologlcal Data–Annual Summary with Comparative Data. 1974" Nattonal Cllmatlc Center, Asheville, N.C

to cos θ_i, where θ_i is the angle between the direction to the Sun (which will be represented with the unit vector $\hat{n}_s$) and the direction normal to the collector (which will be represented with the unit vector $\hat{n}_c$). The function cos θ_i is given simply by

$$\cos\theta_i = \hat{n}_s \cdot \hat{n}_c \quad \textbf{(A-2)}$$

For a fully tracking collector, of course, cos θ_i is always equal to 1 since the collector is always pointing directly at the Sun. Representations of this cosine function for other types of collectors, however, can be quite elaborate since a large number of variables must be considered, With the appropriate choice of geometry, however, the actual calculation can be quite simple. A technique is displayed here which permits a calculation of cos θ_i for all types of tracking collectors. Using equation A-2 requires that $\hat{n}_c$ and $\hat{n}_s$ be expressed **in the same coordinates. The coordinates which are the most convenient are the "collector site coordinates"** illustrated in figures VI II-A-l and VIII-A-2. A glossary of symbols used in computing collector geometry appears in table VI 1 I-A-3. In these coordinates, the z-axis points at the zenith at the collector site, the y-axis points south in the plane of the horizon, and the x-axis points west in the plane of the horizon.

Figure VI II-A.1.– Collector Coordinates Showing the Collector Direction and the Axis of Rotation of the Collector Direction

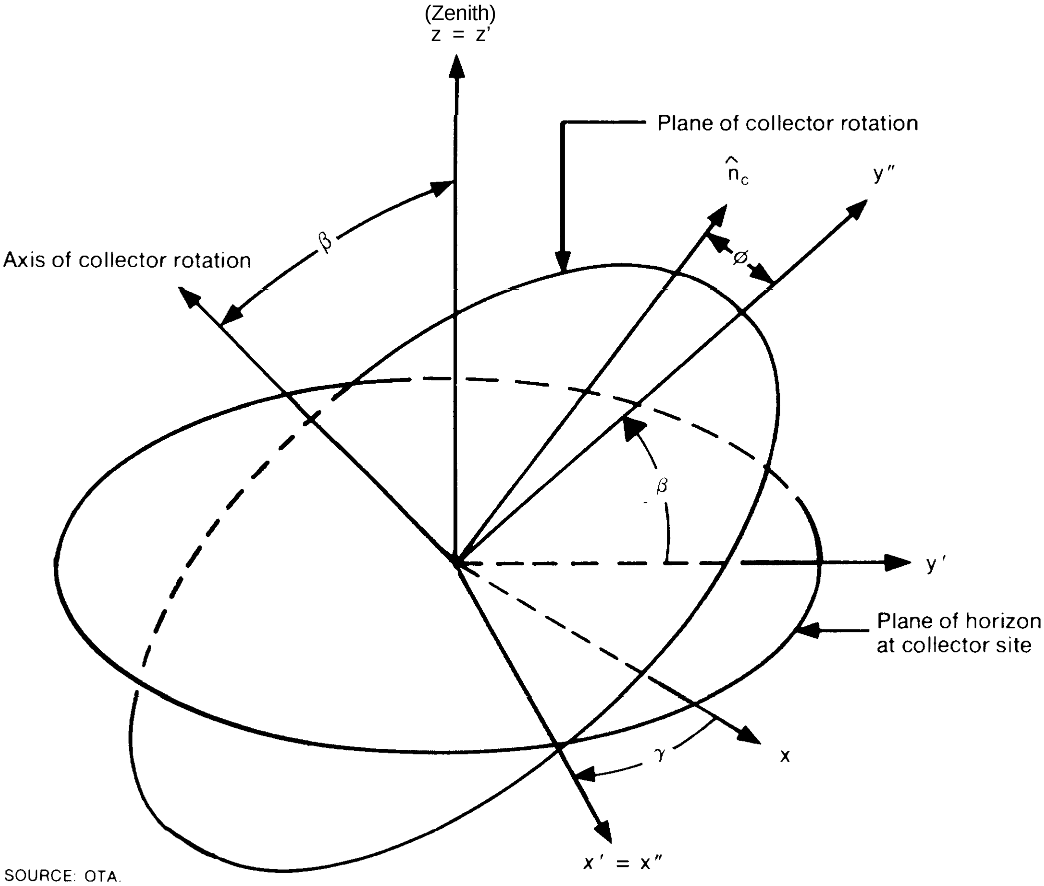

SOURCE: OTA.

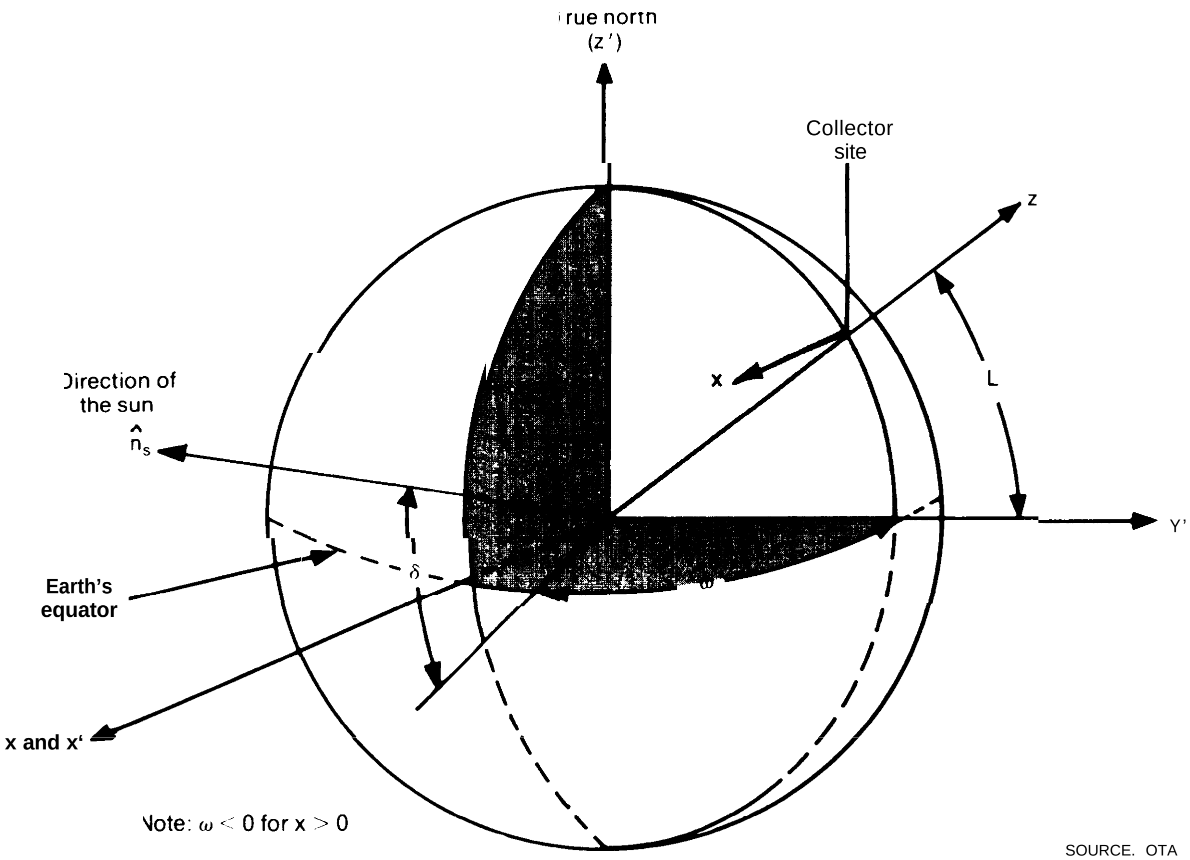

SOURCE. OTA

Table VIII-A-3.—Glossary of Symbols Used in Computing Collector Geometry

(a) *Variables describing the solar position*

L	latitude of the collector site (north is positive)
w	solar hour angle (east is positive, due south is zero)
δ	solar declination (north is positive)
T_n	local standard time on nth day of the year
$T_N(n)$	the hour of solar noon ($\omega = 0$) expressed in clock time using the applicable time zone of the region (eg. eastern standard time) on the nth day of the year
$T_e(n)$	a correction of T_n called the "equation of time" resulting from the fact that the Earth's orbit is not circular, computed for day n
n	the day of the year (0 < n < 365)

(b) *Variables describing the position of the collector*

β	collector tilt angle above the horizontal (positive if tilted south)
γ	direction which the collector faces in the plane of the local horizon (positive if rotated to the east)
φ	angle of rotation about the collector's axis of rotation

The first step is to obtain an expression for the direction of the normal to the collector ($\hat{n}_c$) in the x, y, z coordinates. Figure VIII-A-1 illustrates a completely general collector geometry. The collector direction (n_c) is represented in a set of x'', y'', z'' coordinates which are obtained by two rotations from the x,y, z system: 1) a rotation around the z-axis by an angle γ, and 2) a rotation around the new x'-axis defined by the previous rotation by an amount β. In this double-primed coordinate system

$$\hat{n}_c'' = (\sin \phi, 0, \cos \phi) \qquad \text{(A-3)}$$

where ϕ represents the angle of rotation of a single-axis tracking system where y" is the axis of rotation. The vector can now be transformed simply back to the x,y, z coordinates through two unit rotations which

reverse the rotations by which the x,y, z coordinates were converted to x″ y″ z″ coordinates. With this transformation

$$\hat{n}_c = \begin{pmatrix} \cos\gamma & -\sin\gamma & 0 \\ \sin\gamma & \cos\gamma & 0 \\ 0 & 0 & 1 \end{pmatrix} \cdot \begin{pmatrix} 1 & 0 & 0 \\ 0 & \cos\beta & \sin\beta \\ 0 & -\sin\beta & \cos\beta \end{pmatrix} \cdot \hat{n}_c'' \tag{A-4}$$

$$= (\cos\gamma \sin\phi - \sin\gamma \sin\beta \cos\phi,\ \sin\gamma \sin\phi + \cos\gamma \sin\beta \cos\phi,\ \cos\beta \cos\phi)$$

The second step is to write the Sun position ($\hat{n}_s$) in x,y,z coordinates. This can be done by examining figure VI II-A-2 which defines the "geocentric" coordinates x′ y′ z′. These coordinates are obtained by rotating the collector site coordinates x,y, z through the angle $\pi/2$-L about the x-axis (L is the latitude angle). The z' axis points to true north. In these geocentric coordinates, the Sun's position can be computed simply from its declination angle δ, which changes as a function of the seasons, and the solar hour angle ω, which marks the rotation of the Earth. Using standard polar notation, $\hat{n}_s'$ can be written in geocentric coordinates as follows:

$$\hat{n}_s' = \begin{pmatrix} -\sin(\pi/2-\delta)\sin\omega \\ \sin(\pi/2-\delta)\cos\omega \\ \cos(\pi/2-\delta) \end{pmatrix} \tag{A-5}$$

This vector can be translated into **collector** site coordinates with a simple unit rotation about the x' axis giving

$$\hat{n}_s = \begin{pmatrix} 1 & 0 & 0 \\ 0 & \cos(\pi/2-L) & -\sin(\pi/2-L) \\ 0 & \sin(\pi/2-L) & \cos(\pi/2-L) \end{pmatrix} \cdot \hat{n}_s' \tag{A-6}$$

This achieves the objective of expressing both $\hat{n}_s$ and $\hat{n}_c$ in collector site (x,y,z) coordinates and the cosine function can be computed:

$$\begin{aligned} \cos\theta_i = {} & \hat{n}_c \cdot \hat{n}_s \\ = {} & -\sin\omega\cos\delta[\cos\gamma\sin\phi \\ & -\sin\gamma\sin\beta\cos\phi] \\ & + [\sin L\cos\omega\cos\delta - \cos L\sin\delta] \\ & \cdot [\sin\gamma\sin\phi + \cos\gamma\sin\beta\cos\phi] \\ & + \cos\beta\cos\phi[\cos L\cos\omega\cos\delta \\ & + \sin L\sin\delta] \end{aligned} \tag{A-7}$$

Using equation A-7, the tracking geometry of all collectors can be computed rapidly.

FLAT-PLATE COLLECTORS

The typical flat-plate collector is mounted on a sloping roof which faces south, or nearly so. The general formula" for a fixed fiat-plate collector which is tilted up from the horizontal by an angle β and makes an angle γ with respect to south can be found by simply setting $\phi = 0$ in equation A-7. (Some workers define the tilt angle β with respect to the collector normal $\hat{n}_c$ instead of with the horizontal). When the collectors face due south, γ will also be zero.

SINGLE-AXIS TRACKING COLLECTORS

Single-axis tracking collectors can be mounted many different ways, but two widely used configurations have been used in this study

Polar Mount

The polar mount provides more annual output than other single-axis tracking mounts, but is generally more expensive to construct than mounts where the rotational axis is horizontal. The polar mount can be visualized by imagining a collector which rotates about a horizontal axis running from north to south and then tilting the rotational axis up from the horizontal and toward the south by an amount equal to the latitude angle L (see figure VI **11-8).** The cosine factor for polar-mounted tracking devices can be obtained from equation A-7 by setting $\gamma = 0$

and 13 = L, the latitude angle. Using these values in equation A-7 and minimizing the result with respect to the collector angle of rotation ϕ, it is found that collector output is maximized when $\phi = \omega$. The angle of incidence is then simply the solar declination and

$$\cos \theta_i = \cos \delta \qquad \text{(A-8)}$$

East-West Axis of Rotation

Collectors which rotate about a horizontal axis that runs east to west receive somewhat less sunlight than single-axis polar-mounted collectors, but are sufficiently less expensive that they are more widely used. The cosine factor for this collector geometry can be obtained by setting $\beta = 0$ and $\gamma = \pi/2$. When the resulting equation is maximized with respect to the tracking angle ϕ, it is found that

$$\tan(L - \phi) = \tan \delta \sec \omega \qquad \text{(A-9)}$$

Using A-9 in equation A-7 (with $\beta = 0$ and $\gamma = \pi/2$), and performing some tedious algebra it is found that

$$\cos \theta_i = \pm[1 - \cos^2 \delta \sin^2 \omega]^{1/2} \qquad \text{(A-IO)}$$

Equations of Time

The previous section showed how the collector cosine factor could be computed from information about the solar position (the declination and hour angle) and the collector position. Solar declination can be computed simply since it varies approximately sinusoidally from plus 23.5 degrees to minus 23.5 degrees with the maximum occurring at the summer solstice. Computation of the solar hour angle from local time is complicated by two factors: 1) the time shown on clocks with which the sunlight observations are correlated does not correlate with local solar time **since each time zone covers a large spread of longitudes — the Sun can not be** due south at noon in the entire time zone; 2) the times at which the Sun is directly south are not separated by precisely 24 hours (although the yearly average of these separations is exactly 24 **hours)** since the Earth's orbit is an ellipse and not a circle.

If T_n is the hour of the day measured on the n[th] day of the year in the local time zone (i.e. eastern standard time) and TN(n) is the time at which the Sun points due south on this day (measured in the same local clock time), the solar hour angle can be written on this day as follows:

$$\omega = \frac{2\pi}{24}[T_N(n) - T_n] \qquad \text{(A-11)}$$

The time for solar noon can be computed from the latitude of the collector site (L), the **latitude to which the prevailing time zone is referenced (L_{ref}) (L_{ref} is 120°W for Pacific standard time), and a correction factor $T_e(n)$ computed for each day to account** for the elliptical nature of the Earth's orbit. Using these variables it is found that:

$$T_N(n) = 12 - \left(T_e(n) + \frac{L_{ref} - L}{15}\right) \qquad \text{(A-12)}$$

The equation of time is a complex function of the day of the year and its specification requires solving equations for which no closed solution is possible. **It** can be approximated to limits of precision compatible with the rest of the analysis which will be employed here with four terms of a Fourier series. This series is expanded as a periodic function of the length of the year since the equation must have a period of precisely 1 year Coefficients of this expansion have been computed by the National Bureau of Standards[2] and are illustrated in table **VII I-A-4.** The Fourier formula is, as follows:

$$T_e(n) = \sum_{k=0}^{k=3} (1/60)\left[A_k \cos\left(\frac{2\pi kn}{365.25}\right) + B_k \sin\left(\frac{2\pi kn}{365.25}\right)\right] \qquad \text{(A-13)}$$

'T. Kusuda, *NBSLD Computer Program for Heating and Cooling Loads in Buildings*, NBS I R 74-574, November 1974

Table VIII-A-4.— Coefficients of the Fourier Expansion of the Equation of Time Used in Equation A-15

A_0	-0.0002	B_0	0
A_1	0.4197	B_1	-7.351
A_2	3.2265	B_2	-9.3912
A_3	0.0903	B_3	-0.3361

Diffuse Radiation

The diffuse component of the solar radiation reaching a horizontal surface (I_{dh}) can be computed if information is available about the total energy incident on a horizontal surface (I_{TH}) and the direct normal radiation **(I_D).**

$$I_{dh} = I_{TH} - I_D \cos\theta_H \qquad \text{(A-14)}$$

where θ_H is the angle between the Sun and the horizon directly below the Sun,

This equation, however, carries no information about the distribution of diffuse radiation across the sky and thus there is not a simple way to compute the amount of dif**fuse radiation that can be collected by a device which is not horizontal,** In fact, the distribution of diffuse radiation over the sky **dome varies widely, depending on local weather conditions and on the time of day, It is remarkable, however, that there is very little data in the literature about the distribution which can be expected. In the following discussion, the simplifying assumption that diffuse radiation is distributed uni**formly across the sky dome (the "isotropic sky" assumption) has **been** used, even though it is known that under some conditions the bulk of diffuse radiation emanates from a region in the sky close to the Sun. Very recent work[3] indicates that this is a conservative assumption which understates the radiation on a tilted surface by as much as 7 percent.

Using this "isotropic sky" assumption, it is possible to convert I_{dh} computed in equation A-1 4 into an estimate of I_D-- the intensity of diffuse radiation on a tilted collector. Following Liu and Jordan,[4] it is assumed that the diffuse radiation reaching the collector consists of two parts: (1) a part received directly from the sky (which is assumed to radiate isotropically) and (2) a part reflected from the ground (which is proportional to the fraction of the sky from which radiation could be reflected into the collector). Using these assumptions, it is possible to compute I_d for a collector which has been tilted through an angle β from the horizontal:

$$(I_d/I_{dh}) = \int_{\Omega_s} \cos\theta \cdot d\Omega + \varrho \int_{2\pi-\Omega_s} \cos\theta \cdot d\Omega = \left(\frac{1+\cos\beta}{2}\right) + \varrho\left(\frac{1-\cos\beta}{2}\right) \qquad \text{(A-15)}$$

where Ω_s is the solid angle of the sky seen by the collector and ϱ is the reflectivity of the ground. The reflectivity varies greatly from location to location. It may be very high if the area is covered with snow, and it can be artificially enhanced by placing ponds, or reflective surfaces, in appropriate locations close to the reflectors. For the purpose of this analysis, t is assumed that $\varrho = 0.2$, which is a typical reflectivity of dry ground.

Optical Losses

in addition to the limits imposed by the geometry of tracking, the amount of light which reaches the receiver units in solar collectors is limited by a number of losses due to imperfect optics. These losses include: 1) energy absorbed by transparent covers **over the** receiver; 2) losses when light is reflected from mirror surfaces or transmitted through lenses; 3) errors in pointing a tracking **collec**tor at the Sun; and 4) shading of collectors by adjacent collectors, or (in the case of

[3] Thomas M Klucher, *Variation of Solar Cc// Sensitivity and Solar Radiation on Inclined Surfaces*, presented at the Semiannual Review Meeting, ERDA Silicon Technology Programs Branch, Aug 23-25, 1977, Williamsburg, Va

[4] B Y H Liu and R C Jordan, "The Long-Term Average Performance of Flat-Plate Solar Energy **Collectors,"** *Solar* **Energy** 7, 53(1963)

some tracking units) by other parts of the collector. Designing an optimum collector requires balancing the features which can improve optical efficiency against other design constraints. For example, adding cover glasses can reduce thermal loss but increase optical losses. Increasing the focal length of a concentrating collector can reduce dispersion and transmission losses in lenses, but increases the size of the Sun's image and can add to the bulk and contribute to the wind profile of the collector.[5] Increasing the concentration ratio decreases thermal losses, provides a higher temperature thermal output, or reduces the amount of photovoltaic material required. Higher concentrations increase the significance of pointing errors.

TRANSMISSION LOSSES

Light is lost when it passes through transparent receiver covers. Some light is lost due to surface reflections (from both the front and back surface of the covers), and some light is absorbed by the transparent material. These losses represent the bulk of optical losses in flat-plate collectors and can play a significant role in concentrating collectors which surround a receiver with a glass or plastic cover.

The transmission coefficient for various types of materials is illustrated in table VII I-A-5. These losses are computed only for normal incidence, however, and transmission decreases with increasing angles of incidence. The analysis of the transmission at angles of incidence other than zero can be complex. The following formula fits empirical data with a fair degree of accuracy:[6]

$$T(\theta_i) = \begin{cases} T(0)\ [\cos(\theta_i)]^{1/2} & \text{two covers} \\ T(0)\ [\cos(\theta_i)]^{1/4} & \text{one cover} \end{cases} \qquad \text{(A-16)}$$

here $T(\theta_i)$ is the transmissivity at angle θ_i, and T(0) is the transmissivity for a case where the light is incident normal to the plane of the cover. If diffuse light strikes the collector uniformly from all angles, $T(\theta)$ must be averaged over the section of the sky which is viewed by the collector as follows:

$$\bar{T} = \frac{\int_{\Omega_s} T(\theta)\cos\theta\, d\Omega}{\int_{\Omega_s} \cos\theta\, d\Omega} = \frac{\int_{\beta-\pi/2}^{\pi/2} \cos\phi\, T(\phi)\, d\phi}{1 + \cos\beta} \qquad \text{(A-17)}$$

where Ω_s is the solid ang e of the sky viewed by the collector.

For a horizontal flat-pl ate system receving radiation from an isotropic sky, equation A-1 8 gives:

$$\begin{aligned} T\ (\text{one cover}) &= 0.89\ T(0) \\ T\ (\text{two covers}) &= 0.80\ T(0) \end{aligned} \qquad \text{(A-18)}$$

IMPERFECT REFLECTIONS FROM MIRROR SURFACES

Materials proposed for use as mirror surfaces in concentrating collectors vary greatly in their cost and optical properties. An ideal material would be inexpensive, have a high reflectance, create little dispersion (i. e., a narrow beam of incident light should be reflected without spreading), resist impact from hailstones (no fracturing or denting), and not attract dust. Candidate materials include first-surface glass mirrors (which have high reflectivity but are vulnerable to tarnishing and scratching), second-surface glass mirrors (low-iron glass is preferred to reduce absorption), second-surface bulk acrylic mirrors, annodized aluminum (relatively inexpensive and easy to form but a lower overall reflectivity (60 to 80 percent)), and a variety of metalized plastic films. The plastic films are much less expen-

[5] Gene Nixon, *cast acrylic Fresnel lens solar concentrator* distributed by Swedlow, Inc., obtained by OTA, May 26, 1977.

[6] Empirical expression provided for OTA by Don Watt

Table VIII-A-5.—Transmittance of Transparent Covering Materials Which May be Used in Solar Collectors (Assuming the Solar Spectrum Resulting From Air Mass 1)

Material	Thickness (in.)	Supplier	cutoff wavelength um	Hem is, reflectance	Normal solar transmittance
Quartz	0.125	Sandia Glass Shop	0.26	0.064	0.94
Teflon 100 C . . . ., ...	0.001	Dupont	0.26	0.031	0.93
Pyrex (Corning 7740)	0.134	Sandia Glass Shop	0.36	0.067	0.91
Acrylite ., ., ..., ., ., ...	0.0625	Petterson	0.35	NM†	0.89
	0.125				0.87
Plexiglas "G" ., ., ., ., ., ., .,	0.0625	Petterson	0.35	NM	0.88
	0.219				0.86
Tedlar, polished. . . . . ., . . .	0.004	Dupont	0.31	0.080	0.88
Swedlow centinuous cast acrylic.	0.076	Swedlow	0.33	0.070	0.88
Swedlow coated acrylic,. cell cast	0.273	Swedlow	0.39	0.058	0.85
Israeli collector glazing ., . .	0.092	Peterson	0.31	NM	0.85
Glass for mirror	0.125	Champion	0.31	0.070	0.85

Material	Thickness (in.)	Supplier	cutoff wavelength um	Hem is. reflectance	Hemispherical solar transmittance
Teflon 100 C	0.001	Dupont	0.25	0.031	0.96
Aclar #22A	0.002	Rain hart: Allied Chem.	0.25	0.060	0.94
Corning Ultramicrosheet	0.0045	Butler: Corning	0.30	0.071	0.92
Tedlar, polished.	0.004	Dupont	0.30	0.080	0.91
Lucite 147	0.120	Dupont	0.38	NM†	0.85
Mylar D.	0.010	Dupont	0.33	0.112	0.85
Rhom-Haas Korad A. . . . . std. clear	0.005	Brumleve	0.38	0.088	0.86
Fllon A748, Tedlar coated, ... ,	0.028	Filon Corp.	0.38	0.082	0.84
Kalwall Sunlite Regular	0.040	Kalwall Corp.	0.38	0.079	0.83
Mylar A. . . ., ...	0.005	Dupon	0.38	0.19	0.78
Kalwall Sunlite Premium	0.040	Kalwall Corp.	0.38	0.087	0.79
Swedlow continuous ... cast acrylic	0.076	Swedlow Corp.	0.38	0.070	0.86
Swedlow coated acrylic . (cell cast)	0.273	Swedlow Corp.	0.38	0.058	0.85

†NM = not measured

SOURCE *Solar Total Energy Program Semiannual Report* April 1975 September 1975 SAN D76 0078 Sandia Labs, Albuquerque N Mex April 1976 p 98 99 sive, **but many appear to age rapidly and to attract dust, and currently available materials have relatively low reflectivities. The search** for an optimum reflecting surface will be an important development problem for the next several years.

Figure VI II-A-3 and table VI II-A-6 illustrate the optical properties of a number of different reflecting surfaces. It can be seen that the materials vary greatly both in total reflectivity and in the amount of dispersion introduced. The reflectivity for glass mirrors can be as high as 96 percent, while the inexpensive aluminum reflectors can have reflectivities below 80 percent.

The surfaces also vary in the amount of dispersion which they introduce. Mirrors which introduce large amounts of dispersion cannot be used to achieve high magnification (as is shown quantitatively in the next section). The aluminized 1 Mil Teflon film material shown on figure VII I-A-3, for example, reflects 75 percent of the light incident **on it** into a cone smaller than 4 mrad wide. **The second-surface glass mirror reflects over 90 percent** of its light into a cone less than 2 milt-ad in width.

A final difference between surfaces is the variation of reflectance with the angle of incidence of the incoming light. Class mirrors and first-surface aluminized du Pont experimental film show almost no variation over a wide range of incidence angles, while other materials such as the aluminized **1-3 Mil Mylar-S film have very poor reflectance at** small angles of incidence,[7]

SHADING, BLOCKING, AND END LOSSES

Three additional loss factors must be considered:

[7]R. C Zenter (Boeing Aerospace Co), "Performance of Low Cost Solar Reflectors for Transferring Sunlight to a Distant Collector, " *Solar Energy,* Vol 19, No 1, 1977, pp 15-21

Figure VI II-A-3.—The Specular Reflectance at 500nm as a Function of the Collection Angular Aperture for Several Reflector Materials, Together With Their Solar Averaged Hemispherical Reflectance, $R_s(2\pi)$. Incidence Angle = 20°.

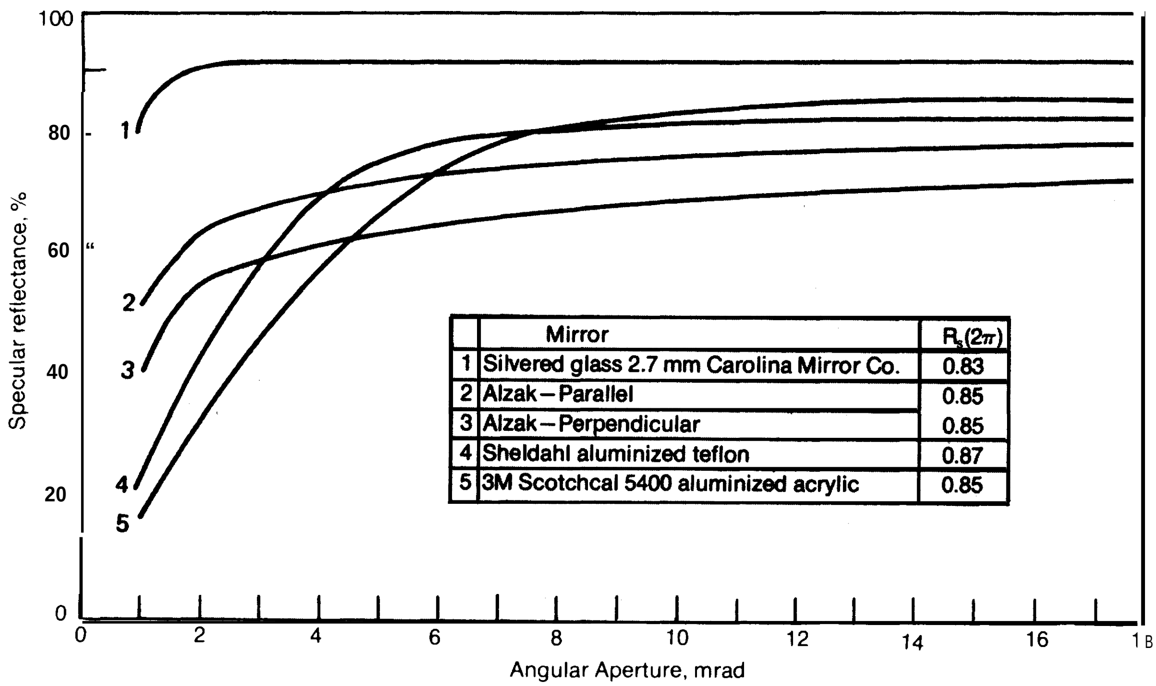

	Mirror	$R_s(2\pi)$
1	Silvered glass 2.7 mm Carolina Mirror Co.	0.83
2	Alzak – Parallel	0.85
3	Alzak – Perpendicular	0.85
4	Sheldahl aluminized teflon	0.87
5	3M Scotchcal 5400 aluminized acrylic	0.85

SOURCE: R. B. Petit and L. G. Rainhart (Sandia Labs, Albuquerque) Private Communication, Sept. 1977.

Table VIII-A-6.—Specular Reflectivities

Material	Supplier	Wavelength (um)	Specular Reflectivity	Cone angle (MRAD) containing 67% of reflected light	Reference
1. Second-surface silvered glass					
A. Laminated glass	Carolina Mirror Co.	**500**	**.92**	**0.15**	**(3)**
B. Corning Micro-sheet, 0.11 mm.	Sandia	**550**	.78	1.1	(4)
C. Corning 0317, no iron, 1.5 mm fu - sion glass.	Carolina Mirror CO.	—	.96	small	(2)
D. Float glass with iron	——	—	**.82**	small	(2)
II. First-surface glass					
A. Double acrylic coat, silver . . .	Sheldahl	**550**	**.93**	**.21**	**(4)**
B. AL/ground glass overcoat		**628**	**.88**	**<1.7**	**(6)**
III. Polished aluminum					
A. ALZAK lighting sheet					
(Parallel to rolling marks)	Alcoa	**505**	.62	.29	(3)
(Perpendicular to rolling marks).		**505**	.56	.42	(3)
B. KINGLUX reflector sheet					
(Parellel to rolling marks). .	Kingston Industries	498	.67	,43	(3)
(Perpendicular to rolling marks).	Kingston Industries	498 Sun	.65 .81	.37 ——	(3)
E. Household foil	——	Sun	.65	——	(8)
V. Metalized plastic films					
A 2nd-surf. alum. FEK-163	3M	**500**	**.86**	**0.90**	**(3)**
B. 2nd-surf. alum. Teflon	Sheldahl	**500**	**.80**	**1.3**	**(3)**
c. 2nd-surf. alum. Teflon laminated to alum. sheet	Sheldahl	**550**	**.87**	**1.2**	(4)
D. Al/nylon, 1st surf ., .	———	Sun	.80	——	(8)
E. A1/Kapton-H, 1st surf. , 0.25 mm		628	.87	5	(6)

References

1 Handbook *of Chemistry and Physics* The Chemical Rubber Co , Ed by R C Weast, 54th Edition, 1973-1974, p E-225
2 L G Rainhard (Sandia Labs, Albuquerque) private communication, Aug 10, 1977
3 R B Petit and B L Butler (Sandia Labs, Albuquerque) *Semiannual Review ERDA Thermal Power Systems, Dispersed Power Systems, Distributed Collectors and Research and Development, Mirror Ma terials and Selective Coatings* SAN D77-01 11, February 1977, p 6
4 *Solar Total Energy Program Semiannual Report October* 1975 *and March 7976 SAND76 0205,* Sandia Labs, Albuquerque, June 1976
5 Test report by Desert Sunshine Exposure Test, Inc , March 4, 1977, rendered to Kingston Industries Corp DSET Order No 17127S
6 R C Zentner (Boeing Aerospace Co), " Performance of Low Cost Solar Reflectors for Transferring Sunlight to a Distant Collector, " *Solar Energy,* Vol 19, No 1, 1977, pp 15-21
7 L Drummeter and G Haas "Solar Absorptance and Thermal Emittance of Evaported Coating s,' *Physics of Thin Films, 2, 1964* Ed by G Haas and R Thun, Academic Press
8 F Daniels (University of Wisconsin, dec) *Direct Use of the Sun Energy* Yale University Press of Ballantine Books, Inc 1964

1. “End losses” of one-axis tracking devices which result from the fact that some part of the light reflecting from a trough or other one-axis tracking unit will miss the receiver surface except during the infrequent occasions when the incident light is directly normal to the collector plane;
2. Shading of collectors by adjacent collectors; and
3. Blocking of the reflected beam of a heliostat by other heliostats

End Losses

If the collector reflecting surface is a flat Fresnel lens or a series of coplanar linear slats, light incident on an area of the collector aperture equal to $FD/\tan\theta$ will miss the receiver surface. (F is the focal length of the optics, D is the collector width, and θ is the angle of incidence of direct sunlight measured with respect to a direction normal to the plane of the collector.) **If the collector length is** L, **then the fraction of the incident light lost in end effects (1’,(0)) is** given by:

$$\Gamma_e(\theta) = \frac{F|\tan\theta|}{-} \qquad \textbf{(A-19)}$$

If the system uses a parabolic trough, the calculation is somewhat more complex since points on the edge of the trough are farther from the focal line than points at the base of the trough. It can be shown that in this case the fraction of the incident light lost in end effects is given by:

$$\Gamma_e(\theta) = [(D/L)\, f/|\tan\theta|] \cdot [1 + 1/(48f^2)] \qquad \text{(A-20)}$$

where f = F/D **is the “f-number” of the optical system.**

Shading **Factors**

The amount of energy lost **when one collector shades an adjacent collector depends** on the exact geometry of the **collector field** and must be computed separately for each case. These losses can be reduced **or eliminated if the collectors are widely spaced, but such separation increases the demand** for land use and can increase piping costs **(in the case of distributed collectors) or add to the demands placed on pointing accuracy (in the case of heliostat designs). In addition, the solar image will be larger from** more distant heliostats, decreasing efficiency, or concentration ratio. A balance must be struck in each application. In many cases, **however, a shading problem will be negligible if the collector surfaces cover less than about one-fourth of the area provided for collectors.**

Heliostats

The shading, blocking, and cosine factors of heliostat fields are complex since the location and pointing angle of each **heliostat in a large field must be analyzed to develop an estimate** of overall system performance. An independent analysis of this problem has not been attempted in this report and the computations of heliostat performance rely on an analysis performed by the University of Houston in connection with the McDonnell Douglas design proposal **for a** 10 MWe pilot plant **for a** 100 MWe central receiver system. The results of this analysis are illustrated in figure VII I-A-4. The curves shown include the effects of atmospheric attenuation for clear days in the southwest United States, and apply to a field optimally designed for a site at *350 N* **latitude.** The designers attempted to design a system which performed well during the periods near dawn and dusk, and which minimized seasonal variations. Mirror spacing is not uniform, but on the average about one-fourth of the area is actually covered with mirrors.

The curves of figure VII I-A-4 indicate the normalized power to the receiver and **include** the cosine factors of the heliostats, shading and blocking effects, a receiver interception factor, and attenuation between the mirrors.

Figure VIII-A-4. —Monthly/Hourly Variation in Available Thermal Power

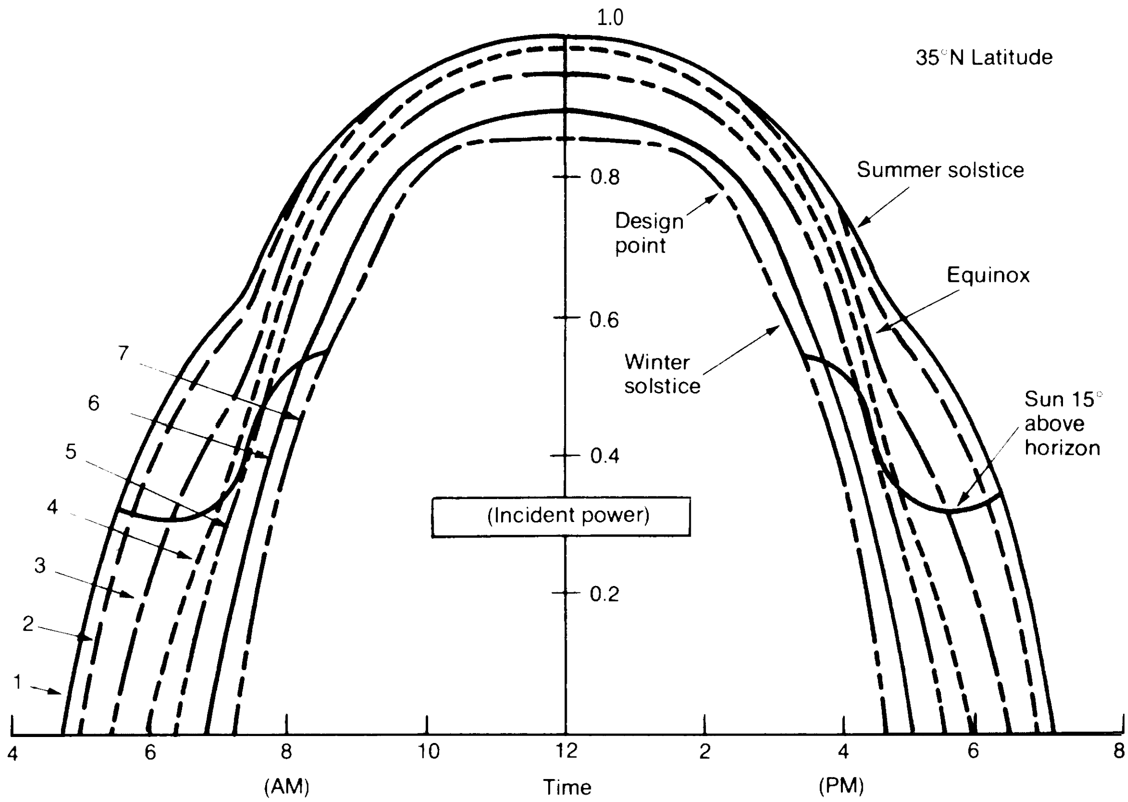

Curve number	**Day** number range when the curve is applicable*
1	158-186
2	127-157 and 187-217
3	97-126 and 218-248
4	66- 96 and 249-278
5	36- 65 and 279-309
6	5- 35 and 310-340
7	1- 4 and 341-365

*January 1 is day #1

SOURCE Raymon W Hallet. Jr and Robert L Gervais. Central Receiver Solar Thermal Power System Phase I 1st Quarter Technical Progress Report McDonnell Douglas Astronautics Company (January, 1976), p 18 MDCG6318

These **curves were** used in the analysis by approximating each curve with a six-line segment polygon adjusted so that the area under the polygon was approximately equal to the area under the curves illustrated. The shapes of the polygons **were also** adjusted to reflect different day lengths at latitudes other than 35° N

Limits on the Geometric Concentration Ratio

The amount of concentration of sunlight possible with a **given set of optics is limited by the pointing accuracy of the tracking system used, by the dispersion introduced into the optics by imperfect reflecting surfaces, and by the finite diameter of the Sun.**

(The intensity of the light actually reaching the absorber will, of course, also be limited by the cosine factor, shading and blocking effects, and the reflection and absorption losses discussed earl ier.)

There is some abiguity about the proper way to define the geometric concentration ratio. I n the **following discussion, geometric concentration ratio (C_g) is defined to be the ratio between the aperture of the collector and the area of the receiver which can be reached by the reflected or refracted sunlight. This definition assumes that the portions of the receiver which can never** be illuminated are well insulated. This definition must be applied with some care in the case of one-dimensional tracking systems since the concentration ratio will not be equal to the ratio between the solar energy reaching the mirror or lens surface and the light reaching the collector absorber (assuming perfect optics), except when the Sun's direction is directly normal to the plane of the collector. At all other times, the effective geometric concentration ratio for a perfect collector is equal to the geometric concentration ratio multiplied by the shading factor $1 - \Gamma_e(\theta)$.

If the optical properties of the system are perfect, the only limit on the geometric concentration ratio will be the angular diameter of the Sun. The Sun's diameter (γ_s) varies from 9.16 milrad to about 9.46 milrad, changing as the Earth-Sun distance varies over the year. The limits which this imposes on the concentration ratios possible are illustrated for three different concentrating systems in figure VII I-A-5. The solar image reflected (or transmitted) from an extreme edge of the lens or mirror has a width of $R_m\alpha_s$ and the solar image reflected (or transmitted) from the center of the lens or mirror has a width of approximately $F\alpha_s$ (where F is the focal length of the optical system). It can be seen that the intensity of the image will be greater in the image center. This can create difficulties if "hot-spots" place high stresses on small parts of the receiver, and nonuniform illumination can reduce the performance of photovoltaic cells. With careful design the impact of these effects can be reduced. For example, the facets of a Fresnel lens or mirror can be adjusted to spread the image to create a uniform illumination on the receiver surface. Measurements performed on a cast acrylic Fresnel lens designed by Swedlow, Inc., are shown in figure VII I-A-6. Careful mirror design or the use of a secondary mirror near the focal point can also minimize the problem of uneven illumination. A precise computation of the intensity distribution of the solar image requires compensation for the fact that the luminosity of the Sun varies over the solar disk. [8]

The size of the solar image reaching the receiver in any practical system will be larger than the angular diameter of the Sun because of dispersion introduced by imperfect reflecting or transmitting surfaces, by imperfect concentrator shape, and because of imperfect tracking. In addition, atmospheric dispersion (e. g., hazy sky) can increase the apparent diameter of the Sun by a factor of 2 or more.

The dispersion introduced by different types of reflecting surfaces was illustrated in figure VII I-A-3. I n the following calculations, the cone angle containing 90 percent of the reflected light intensity is called α_d. Lenses have some advantage in minimizing dispersion since an imperfection in a mirror surface which has the effect of tilting the mirror surface by an angle A above the ideal mirror angle will result in an error **2A** in the angle at which light is reflected. A lens with a similar error at each surface typically results in an angular error of less than 2A, depending on the index of refraction of the lens and the angle between the lens surfaces.

Tracking errors can be treated with fair accuracy by simply assuming that the solar image is spread by tracking errors by an

'D. L. Evans (Arizona State University), "On the Performance of Cylindrical Parabolic Solar Concentrators with Flat Absorbers, " *Solar Energy,* **Vol. 19, No, 4,1977,** pp **379-385.**

Figure VIII-A-5.—The Solar mane on Three Typical Concentrating Collectors

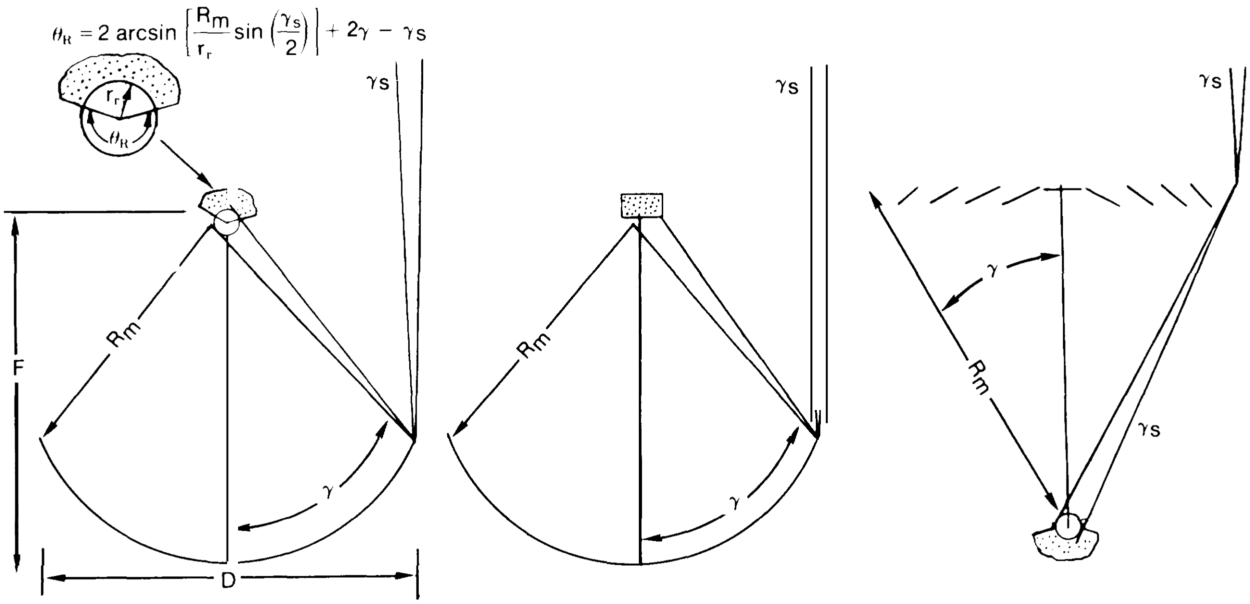

Parabolic Trough with Cylindrical Absorber

Parabolic Trough with Flat Absorber

Flat Fresnel Lens with Cylindrical Absorber

SOURCE OTA

angle *at.* The angle a_t will be chosen to be twice the angle between the ideal collector direction and the actual collector direction, which is exceeded less than 5 percent of the time when the collector is operating. An estimate of the maximum concentration possible given tracking and optical dispersion effects can be made by simply replacing γ in equation A-23 with a where a is given by:

$$a = a^2_s + a^2_d + a^2_t$$

If **chromatic aberation is an important effect, a_d should be increased accordingly. A simple tracking system can achieve a pointing accuracy such that a_t is below about 0.5 degrees or 8.6 milrad.** Such a system could have a dispersion angle of 0.6 degrees or **10.5 milrad. A carefully constructed system** can have a combined error (2δ), due to **dispersion and tracking, of 6 milrad.**[9] **If the mean solar diameter is used, these cases** give a = 16.5 milrad (imprecise optics and tracking); a = 11.1 milrad (precise optics and tracking).

The calculation of the concentration ratio C_g, as defined earlier, must begin with a calculation of the area of the receiver required to capture some desired fraction of the available sunlight. It is easiest to begin by computing the maximum distance from the lens or mirror to the focal point of the collector. This length, which is called R_m, can be calculated as follows:

$$(R_m/D) = \begin{cases} f\sqrt{1 + 1/(4f^2)} & \text{flat lens or segmented mirror} \\ f\,[1 + 1/(4f)^2] & \text{parabolic mirror} \end{cases} \quad \text{(A-21)}$$

where f = F/D and the other variables used are defined in figure VII I-A-5, It will also be necessary to compute the half rim-angle γ (see figure VIII-A-5). This variable can be computed from R_m/D as follows:

[9] Raymon W Hallet, **Jr , and Robert L** Gervais, **Cen-***tral* **Receiver Solar Thermal** *Power System* **Phase** *1, Final* **Report, McDonnel I Douglas Astronautics Company (1 977) SAN 1108**

Figure Vlll-A-6.—Characteristics of the Image of Acrylic Fresnel Lenses Designed by Swedlow Inc. for Solar Applications

Intensity distribution **at the focus of an acrylic fresnel lens designed for** one-axis **concentration on a linear thermal receiver.**

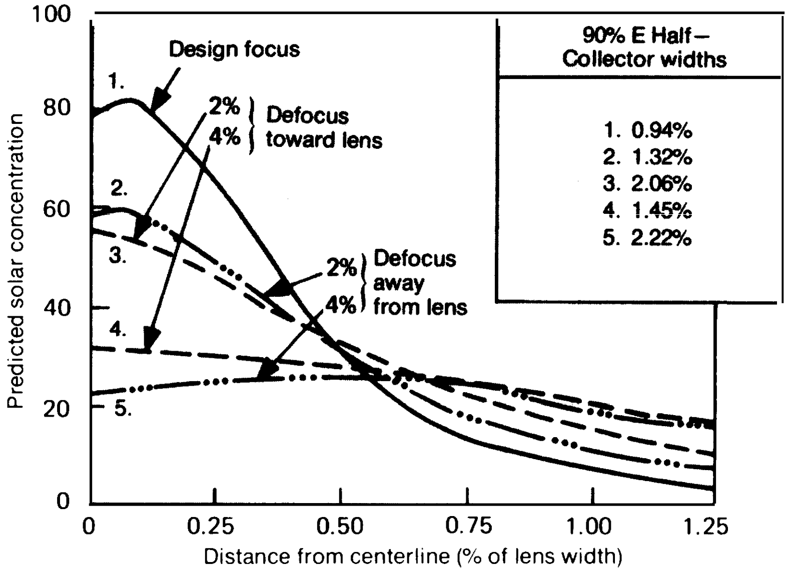

Intensity distribution at the focus of an acrylic fresnel lens designed for **two-axis concentration on a photoelectric device.**

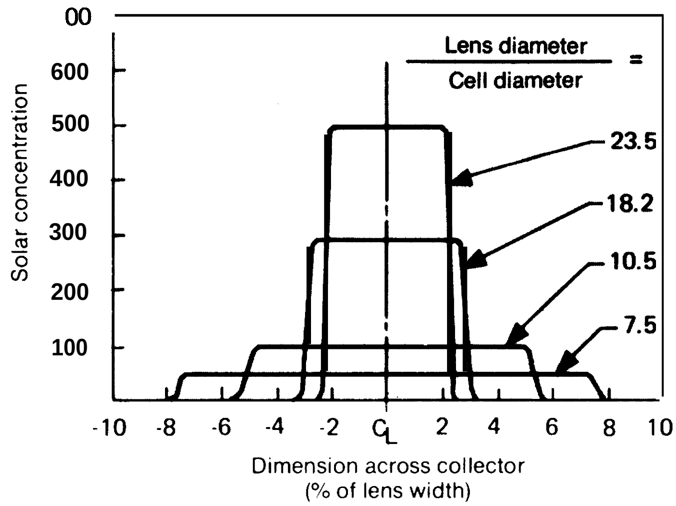

SOURCE Nixon Gene Cast Acrylic Fresnel Lens Solar Concentrator paper distributed by **the** Swedlow Inc obtained by OTA May 26, 1977 pages 27 and 22

$$\gamma = \sin^{-1}(D/2R_m) \qquad \text{(A-22)}$$

With perfect tracking and optics, all of the sunlight incident on a one-axis tracking collector could be captured by a flat receiver with area A_r where

$$A_r = LR_m\,\gamma/\cos\gamma + (\text{terms of order } \gamma^2) \qquad \text{(A-23)}$$

In computing the effective receiving area for a receiver with a circular cross section, it is assumed that the portions of the receiving tube which are never illuminated by the Sun are covered with an insulating material of sufficient quality that losses through the insulation are negligible, The angle measured from the center of the circular receiving tube which can be illuminated (θ_R) is given by

$\theta_R = 2\sin^{-1}[(R_m/r_r)\sin(\alpha/2)] + 2\gamma - \alpha \simeq \pi + 2\gamma - \alpha$ when the concentration ratio is maximized by setting the receiver radius $r_r = R_m\alpha/2$. The area of the receiver in this case is given by

$$A_R = L\alpha R_m \theta_R/2 \qquad \text{(A-24)}$$

Using equation A-23 or A-24, it is now possible to compute the geometric concentration ratio simply with $C_g = LD/A_R$. Tables VIII-A-7 and VIII-A-8 illustrate C_g for a variety of different assumptions. The concentration ratios for the two-axis tracking systems are simply the square of the concentration ratios for the one-axis tracking system.

Net Sunlight Available

The sunlight reaching the receiving surface or absorber (I_s) for a nonconcentrating collector includes both direct and diffuse sunlight and can be expressed as:

$$I_s = \varrho\,(1-\Gamma_e)\,(1-\Gamma_s)\left[I_D T(\theta)\cos\theta - \bar{T}(I_{TH} - I_D\cos\theta_H)\left(\frac{1+\cos\beta}{2} + \varrho_g\,\frac{1-\cos\beta}{2}\right)\right] \qquad \text{(A-25)}$$

Γ_e = fraction of energy lost as end losses
Γ_s = fraction of energy lost in shading and blocking
ϱ = reflectivity of mirrors
$T(\theta)$ = transmissivity of cover plates
θ = angle of solar incidence on collector
θ_H = angle between zenith and Sun
β = collector tilt above horizontal
ϱ_g = surface reflectivity of the ground
I_D = direct sunlight
I_{TH} = total horizontal sunlight

As the concentration ratio increases above one, the fraction of the diffuse radiation intercepted by the collector which reaches the receiver surface drops rapidly, and for concentration ratios above 10, the diffuse sunlight can generally be neglected, leaving

$$I_s = \varrho(1-\Gamma_e)(1-\Gamma_s)\,I_D T(\theta)\cos\theta \qquad \text{(A-26)}$$

Thermal Losses

Not all of the solar energy reaching the receiving element of a solar collector can be removed as useful energy since some of the energy reaching the receiver will be reflected from the absorbing surfaces of the receiver and some of the absorbed energy will be conducted or reradiated back to the atmosphere. As shown earlier, the thermal loss effects are usually much more significant for flat-plate collector systems with relatively large receiver surfaces than they are for concentrating systems with relatively

Table VIII-A-7.—Maximum Possible Geometric Concentration Ratios at Perihelion (Perfect Optics $\gamma = \gamma_S$)

	1-D Concentrator					2-D Concentrator		
f-number of optics (F/D)	Flat receiver, parabolic trough	Tubular receiver, parabolic trough	Flat receiver, flat Fresnel concentrator	Tubular receiver, flat Fresnel concentrator	Flat receiver, parabolic dish	Spherical receiver, parabolic dish	Flat receiver, flat Fresnel concentrator	Spherical receiver flat Fresnel concentrator
.2	...	66.	73.	71.	...	4311.	5315.	5072.
.4	83.	71.	103.	67.	6935.	5016.	10636.	4496.
.6	106.	64.	104.	60.	11173.	4061.	10811.	3584.
.8	99.	55.	95.	53.	9793.	3072.	9029.	2781.
1.0	88.	48.	85.	47.	7706.	2342.	7152.	2170.
1.2	77.	43.	75.	41.	5991.	1824.	5634.	1720.
1.4	69.	38.	67.	37.	4713.	1453.	4484.	1387.
1.6	61.	34.	60.	34.	3772.	1182.	3623.	1138.
1.8	55.	31.	55.	31.	3073.	978.	2972.	949.
2.0	50.	29.	50.	28.	2544.	822.	2475.	802.
2.2	46.	26.	46.	26.	2137.	700.	2088.	686.
2.4	43.	25.	42.	24.	1818.	604.	1782.	592.
2.6	40.	23.	39.	23.	1564.	525.	1537.	517.
2.8	37.	21.	37.	21.	1359.	461.	1339.	455.
3.0	35.	20.	34.	20.	1191.	408.	1175.	403.
3.2	32.	19.	32.	19.	1052.	364.	1040.	360.
3.4	31.	18.	30.	18.	936.	326.	926.	323.
3.6	29.	17.	29.	17.	838.	294.	830.	291.
3.8	27.	16.	27.	16.	754.	266.	748.	264.
4.0	26.	16.	26.	16.	682.	242.	677.	241.

SOURCE. OTA

Table VIII-A-8.—Maximum Possible Geometric Concentration Ratios (Imprecise Optics and Tracking γ = 16.5 Milrad)

	1-D Concentrator				2-D Concentrator			
f-number of optics (F/D)	Flat receiver, parabolic trough	Tubular receiver parabolic trough	Flat receiver, flat Fresnel concentrator	Tubular receiver, flat Fresnel concentrator	Flat receiver, parabolic dish	Spherical receiver, parabolic dish	Flat receiver, flat parabolic concentrator	Spherical receiver, flat Fresnel concentrator
.2	....	36.	41.	40.	•	1330	1640	1570.
.4	46.	39.	57.	37.	2140,	1553.	3283.	1392.
.6	59.	35.	58.	33.	3449.	1257,	3337.	1110.
.8	55.	31.	53.	29.	3023.	952	2787	861.
1.0	49.	27.	47.	26.	2378.	725.	2207.	672.
1.2	43.	24.	42.	23.	1849.	565.	1739.	533.
1.4	38.	21.	37.	21.	1455.	450.	1384	430.
1.6	34.	19.	33.	19.	1164.	366	1118	353.
1.8	31.	17.	30.	17.	948.	303.	917.	294.
2.0	28.	16.	28.	16.	785.	255.	764	248.
2.2	26.	15.	25.	15.	660.	217	644	212.
2.4	24.	14.	23.	14.	561.	187.	550.	184.
2.6	22.	13.	22.	13.	483.	163.	474,	160.
2.8	20.	12.	20.	12.	419.	143,	413	141.
3.0	19.	11.	19.	11.	368.	126.	363	125.
3.2	18.	11.	18.	11.	325	113.	321.	111.
3.4	17.	10.	17.	10.	289	101	286	100.
3.6	16.	10.	16.	10.	259,	91	256	90.
3.8	15.	9.	15.	9.	233.	83.	231	82.
4.0	15.	9.	14.	9.	211	75	209	75.

SOURCE OTA

small receiver surfaces. The thermal loss effects have been treated extensively in a number of recent publications[10 11 12 13 14 15] and no attempt is made to reproduce the analysis presented in these works. All that is done here is to summarize the results which are directly relevant to the analysis of this study.

THERMAL LOSSES AND HEAT COLLECTED

Two different, but rather simple, expressions were used to compute the thermal losses, For some cases, the fluid flow rate f_r was fixed. The heat Q_c collected per unit area of collector is then

$$Q_c = F_r [I_s - U_L (T_i - T_a)] \qquad \text{(A-27)}$$

Here U_L is a thermal loss coefficient (the effective conductivity between the heated fluid and the atmosphere). F_r is the "collector heat removal factor''" which accounts for the use of the fluid inlet temperature T, instead of the mean absorber temperature in the calculation. T_a is the outdoor air temperature.

The other case modeled assumed that the flow rate is varied so the fluid outlet temperature T_o remains constant. The heat collected is then

$$Q_c = I_s - \frac{U_L([(T_i + T_o)/2] - T_a)}{1 + U_L/k_e} \qquad \text{(A-28)}$$

Here k_e is the thermal conductivity between the absorber surface and the fluid, For the concentrating collectors considered, U_L/k_e is less than 0.01 and can be ignored. For heliostats, U_L was based on the outlet temperature rather than the mean temperature.

Typical thermal loss coefficients for a variety of collectors are shown in table VII I-A-9.

It should be noted that the thermal loss term of equation A-27 would be divided by the concentration ratio to obtain the heat lost by concentrating collectors. The expressions used for determining the performance of photovoltaic collectors are somewhat more complicated and are discussed in chapter X.

Detailed *Calculation of Flat. Plate Collector Output*

This section presents methods for computing the output of flat-plate collectors which assume that the thermal loss coefficient U_L is constant and a method which explicitly considers the dependence of U_L on the wind velocity, collector tilt, absorber temperature, and air temperature. The results show that the approximations used with U_L constant are adequate for the long-term system performance which is central to this study.

There are three primary sources of heat loss from the receiver of a solar collector:

1. Radiation – Any hot body radiates energy at the rate of $\epsilon\sigma T^4$, where T is the temperature of the body in degrees Kelvin, ϵ is the emissivity of the radiating surface, and σ is the Stefan-Boltzmann constant:

   $(5.67 \times 10^{-8} \text{Watt/m}^2\text{-K}^4)$.

2. *Conduction* – Heat flows from the

---

[10] John A Duffie ancf William A Beckman, op cit chapters 4-8

[11] Frederick F Simon, *Flat-Plate Solar-Collector Performance Evaluation with a Solar Simulator as a Basis for Collector Selection and Performance Prediction*, NASA TM X-71 793, presented at 1975 ISES Meeting, Los Angeles, Calif

[12] M W Edenburn, *Performance of a* Focusing Cylindrical *Parabolic Solar Energy Collector:* Analysis and *Computer* Program, SLA-74-0031, Sandia Laboratories, April 1974

[13] G W Treadwell, W H McCulloch, and R S Rusk, *Test* Results *from a Parabolic-Cylindrical Solar Collector*, SAND 75-5333, Sandia Laboratories, July 1975

[14] Raymon W Hallet, Jr, and Robert L Gervais, *Central Receiver Solar Power System, Phase 1– Final* Report Pl/et *Plant Preliminary Design* (MCDC 6040), pp 310, 337,366, January 1976

[15] Giovanni Francla, "Large Scale Central Receiver Solar Test Facilities" *Proceedings*, Int Seminar on Large Scale Solar Energy Test Facilities, Las Cruces, N Mex , Nov 18-19, 1975

[16] John A Duffie, op cit pp 146-151

Table VIII-A.9.—Typical Thermal Loss Coefficients

Collector type	(kW/m²°C)	Temperature range	Reference
1 cover flat plate . . .	.0074	< 150° F (< 66" C)	1
2 cover flat plate .	.0046 -.0063	< 200° F (< 93" C)	1
2 cover flat plate, selective absorber. .	.0032 -.0046	< 250° F (<1210 C)	1
Tubular flat plate. .	.0011 -.002	< 250° F (<121 "C)	1,2
Parabolic trough, unglazed.	.025	140°-3500 F (60°-1770 C)	3
Parabolic trough, glazed, sel. absorber, no vacuum.	.009	250°-6000 F (121 °-316°C)	4
Heliostat	.03	9000-1 ,100° F (482°-5930 C)	5,6
Parabolic dish	.076	1,4000-1 ,500° F (760°-8160 C)	7

1 Simon, Frederick F , op cit
2 *Air Conditioning & Refrigeration Business*, July 1976 data for KTA collector
3 Acurex Aerotherm, "Technical Note, Concentrating Solar Collector Model 3002-01 ," received by OTA, 1977
4 Acurex Aerotherm, "Model 3001 High.Temperature Concentrating Solar Collector, " specifications received by OTA, 1977
5 Hallet, Raymon W , Jr Ibid
6 Franc la, Giovanni, Ibid
7 Estimate based on T'scaling of heliostat value

heated collector surfaces through insulation, covering glass, and structural supports to the atmosphere.

3 Convection – Circulation of the air be**tween** the collector plates or motion of air outside the top cover of the collector causes thermal losses. Such circulation is generally present due to gravity, **even in enclosed** spaces. Such losses can, of course, be greatly reduced if the space between the receiver surface and covers is evacuated.

For long-term modeling, the heat loss can be treated as proportional to the difference between the average absorber surface temperature and the ambient air temperature; i.e., the heat loss per unit absorber surface area is $U_L \Delta T$ where U_L is the effective conductance between the absorber surface and the atmosphere and includes losses due to al l three processes mentioned above.

When the collector inlet and outlet fluid temperatures T_i and T_o are known, the **useful thermal output (Q_c) can be given as:**

$$Q_c = A_c I_s - \frac{(U_L/C_R)[(T_i + T_o)/2 - T_a]}{1 + U_L/k_e} \tag{A-29}$$

where

A_c = **collector** aperture area
I_s = sunlight intensity reaching the collector (see equation A-25)
U_L = thermal loss coefficient per unit area of absorber surface
C_r = concentration ratio of the optical system used
T_a = the ambient air temperature
k_e = heat transfer coefficient between the absorber surface and the fluid,

Equation A-29 makes the implicit assumption that the temperature of the surfaces of the absorber and the fluid temperatures vary l i nearly over the area of the collector. The actual distribution of temperatures across the area of the collector depends on

the details of the construction of the device (placement of the tubes, the heat-conducting properties of metal surfaces, etc.). Several recent papers have examined this problem with **some care,**[17 18 19] **A simple technique for approximating this complicated calculation which was** used in the analysis conducted for this study relies on defining a correction factor, Fr.

This **correction** factor, sometimes called the "heat removal factor, " is defined to be the ratio of the useful thermal output of a collector (Qc) to the **useful output of the collector, assuming that the entire collector absorber surface was held at the inlet temperature (T,):**

$$F_R = \frac{f_r C_p (T_o - T_i)}{I_s - (U_L/C_R)(T_i - T_a)} \quad \textbf{(A-30)}$$

where f_r is the mass velocity of the fluid moving through the collector and C_P is the specific heat of the collector fluid. The heat removal factor defined in this way actually changes slightly throughout the year as a function of operating conditions, but it can be shown that in most cases of practical interest, these changes are negligibly small when T_o- Ti is only a few "C. Assuming that F_R is a constant, the collector output can be given **as follows:**

$$Q_c = F_R A_c [I_s - (U_L/C_R)(T_i - T_a)] \quad (A\text{-}31)$$

Techniques for computing F_R for different types of collector geometries are discussed **in detail** in Duffie.[20]

A similar approximation which can be used to evaluate the performance of collectors covered with photovoltaic **cells is discussed** in chapter X. The values of U_L actually used in the analysis were based on the empirical performance data summarized **in table VII** I-A-IO.

An iterative Solution to Collector Heat Loss

A **typical flat-plate collector is** shown in figure VI II-A-7 and **is used to illustrate the detailed method** used to compute heat losses. **The system is characterized** by five temperatures:

T_1 = **the temperature of the absorber plate**
T_2 = **the temperature of the inside cover**
T_3 = **the temperature of the outside cover**
T_4 = **the ambient air temperature**
T_5 = **the effective black** body temperature of the atmosphere

[17] F F **Simon,** *F/at-P/ate Solar Collector Performance Evaluation Performance Prediction,* **presented at the** ISES **Meeting, Los Angeles, Cal If , July 28-Aug 8, 1975**
[18] Duffie, **op** cit **, pp 138-153**
[19] E **M Sparrow and R J Krowech,** *Journal of Heat Transfer,* Vol **99, 1977, pp 360-366**

[20] **Duffie, op cit., pp 146-151**

Table VIII-A-10.—Ratio of Collector Output When "Average" U-Value Used to Output of Collector With Variable U-Value for Flat-plate Collectors in Omaha With Tilt Angle— Latitude

Collector type	Inlet temper-ature	"Average" U-value (kW/m²°C)	Jan	Feb	Mar	Apr	May	Jun	Jul	Aug	Sep	Oct	Nov	Dec	Annual
1 cover	90° F(32°C)	,0069	.946	.954	.977	.999	1.007	1.005	1.005	1.003	1.002	.999	.992	.970	.996
1 cover	120°F(49°C)	.0072	.900	.913	.964	1.006	1.033	1.024	1.019	1.022	1.014	1.003	.993	.942	1,004
2 cover	120°F(49°C)	.0041	.945	.956	.974	1.001	1.015	1.012	1.011	1.012	1.007	1.002	.989	.967	.998
2 cover, selective absorber	1 50° F(66°C)	.0025	.978	.983	.991	1.004	1,014	1.012	1.011	1.011	1.007	1.004	.999	.986	1.003

SOURCE OTA

Figure VIII-A-7. —Geometry of a Simple Flat-Plate Collector

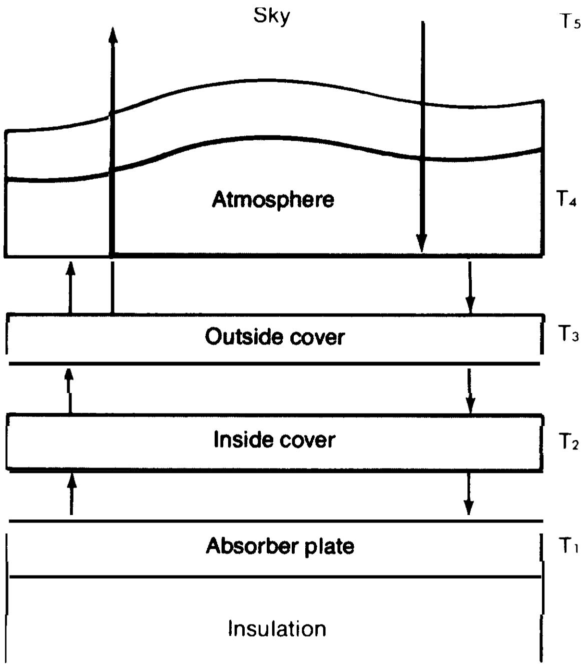

(The typical temperature drop occurring across a glass cover is less than 10 C, so each cover is assumed to be at a single temperature.) The receiver and first cover are separated by a distance d_{12} and the inside and outside covers are separated by a distance d_{23}. **In equilibrium, the heat flowing from the absorber to the first cover must equal** the **heat flow between the two cover plates** which must, in turn, **equal the heat flowing from the top plate into the atmosphere. If** the heat flowing from surface i to surface j is **called** Q_{ij}, **the heat** flows can be expressed as follows:

$$
\begin{aligned}
Q_{12}(C_R/A_c) &= \epsilon_{12}\sigma T(T_1^4 - T_2^4) + h_{12}(T_1 - T_2) \\
&= k_{12}(T_1 - T_2) \\
Q_{23}(C_R/A_c) &= \epsilon_{23}\sigma T(T_2^4 - T_3^4) + h_{23}(T_2 - T_3) \\
&= k_{23}(T_2 - T_3) \\
Q_{34}(C_R/A_c) &= \epsilon_{34}\sigma T(T_3^4 - T_5^4) + h_{34}(T_3 - T_4) \\
&= k_{34}(T_3 - T_4)
\end{aligned}
\qquad \text{(A-32)}
$$

Here h_{ij} are the effective convective/conductive heat transfer coefficients (it being assumed that convective and conductive losses are linear with the temperature difference) and ϵ_{ij} is the effective emissivity for radiative heat transfer between the two surf aces.

The coefficient ϵ_{ij} can be computed by supposing that energy radiated from one surface with temperature T_i and emissivity ϵ_i is all incident on a second surface with temperature T_j and emissivity ϵ_j. Of the energy initially incident on surface *j*, a fraction ϵ_j will be absorbed and $(1-\epsilon_j)$ will be reflected. An infinite **series can thus be constructed and it can be shown that the net heat transfer rate** per unit area is given by

$$\epsilon_{ij}(T_i^4 - T_j^4) \quad \text{where} \quad \epsilon_{ij} = [1/\epsilon_i + 1/\epsilon_j - 1]^{-1} \qquad \text{(A-33)}$$

The convective/conductive heat transfer coefficients are much more difficult to evaluate since a number of effects can contribute to these losses and since the convective effects will depend on the precise geometry and orientation of the collector. The coefficients which apply to the spaces inside the collector (h_{12} and h_{23}) are usually given by:

$$h_{ii} = Nu\, K_a/d_{i,i+1} \quad i = 1,2 \qquad \textbf{(A-34)}$$

where *Nu* is the Nusselt number of the process (the ratio of the convective heat transfer to the conductive transfer) and K_a is the conductivity of air. The problem then **becomes one of establishing an appropriate** Nusselt number for **the process.** Hollands, **et** al.,[21] have **suggested the following (basically empirical formula):**

$$Nu = 1 + 1.44\left(1 - \frac{1708}{R\cos\beta}\right)\left(1 - \frac{1708(\sin 1.8\beta)^{1.6}}{R\cos\beta}\right) + \left[\left(\frac{R\cos\beta}{5830}\right)^{0.33} - 1\right] \qquad \text{(A-35)}$$

[21]K.G. T Hollands, **et al.,** *Journal of Heat Transfer,* **Vol. 98, May 1976, pp. 189-193,**

R = Rayleigh number
= $[gB\Delta T d^{3}_{i,i+1}]/\nu\alpha$

B = thermal expansion coefficient of air
ν = kinematic viscosity of air
g = gravitational acceleration
α = thermal diffusivity of air
β = angle of tilt from horizontal
ΔT = $T_{i+1} - T_i$

The symbol $\{x\} = [(|x| + x)/2]$

Outside of the collector, convection will be affected by the wind and the computation of h_{34} must include this effect.

Recent work[22] suggests that for a wide range of wind conditions, the convective/conductive heat transfer coefficient outside the collector may be taken as:

$$h_{34} = \text{larger of} \begin{cases} 1.08\, Pr^{0.33} Re^{0.5} K_a/d \\ 0.14\,(R\sin\beta)^{0.33}\, K_a/d \end{cases} \qquad \text{(A-36)}$$

Pr = Prandtl number = $C_p\mu/K_a$
Re = Reynolds number = Vd/ν
d = hydraulic diameter = 4 ×(collector area)/(collector perimeter length)
C_p = specific heat of air
V = wind velocity

The bottom expression in equation A-36 (due to Lloyd, *et al.*[23]) corresponds to turbulent free convection.

If the temperatures T_1 through T_5 and coefficients ϵ_{ij} and h_{ij} are known, k_{ij} can be determined from equation A-34 and the thermal loss coefficient U_L is

$$U_L = [(1/k_{12}) + (1/k_{23}) + (1/k_{34})]^{-1} \qquad \text{(A-37)}$$

A correction to equation A-29 must be made for losses through the back and sides of the collector, but these corrections are not shown explicitly in the following discuss ion since they are easy to compute once the temperatures in the collector are known,

Since the heat loss coefficients k_{ij} have a weak but complicated temperature dependence, it is usually not possible to obtain a closed expression for U_L. The most convenient technique for computing U_L is to solve an algorithm for the expression using a digital computer. One such technique is presented below,

The solution is initiated with the assumption that the average temperature of the receiving surface (T_i) is equal to the inlet fluid temperature T, and that the temperature rise across the thickness of the collector is equally divided between the two air spaces (i.e., $T_2 = T_1 + (T_1 - T_4)/3$ and $T_3 = T_2 + (T_1 - T_4)/3$). These temperatures can then be used to compute the heat loss coefficients k_{ij} which can in turn be used to obtain a new estimate for the temperatures T_3 and T_2 using equation A-32. These new temperatures can then be used to compute a new set of approximations to k_{ij}. The cycle is continued until successive values of T_2 and T_3 satisfy a convergence criteria. When the desired convergence is achieved, the parameter U'_L can be computed, including the side and back losses. This U'_L can be used to compute the collector output:

$$Q_c = A_c F_R [I_s - U'_L(T_i - T_4)] \qquad \text{(A-38)}$$

and the output temperature of the fluid moving through the collector is then $T_o = T_i + Q_c/MC_p$ where M is the mass flow rate and C_p is the specific heat of the fluid, With this estimate of TO, a new estimate of the average temperature of the collector surface can be computed as $(T_i + T_o)/2 + Q_cC_R/h_fA_c$ where h_f is the heat transfer coefficient between the fluid and the absorber surface. The procedure for computing U_L for a given ambient temperature and plate temperature can be used again to obtain a new estimate of U_L. This series can be continued until a convergence criteria for the average temperature of the collector surface is satisfied. A final value of U'_L can then be computed which meets all of the specified boundary conditions.

---

[22] E M Sparrow, University of Minnesota, private communication, Febr 25, 1977

[23] J R Lloyd, E M Sparrow, and E R G Eckert, *Int. Journal of Heat and Mass Transfer*, 15,457-473, (1972)

An Approximate Solution

Since the procedure just described is quite lengthy and quite expensive to execute on a computer, an approximation was used to compute the heat loss in the analysis of integrated systems conducted for this study. The approximation was simply to use equation A-29 or equation A-31, depending on whether the system was modeled with a fixed-outlet temperature T_o or with a fixed-flow rate f_r. This equation was used with an empirically derived value for U_L which was assumed to be constant throughout the year. Measured values of U_L for a variety of different collector designs are shown in table VII I-A-IO.

Table VIII-A-IO compares the monthly output of collectors calculated assuming a U-value independent of temperature with the collector output calculated using the variable U-value procedure of the previous sect ion. Computation of the variable U_L-values using the iterative solution included all corrections discussed in the previous section: it assumed $F_R = 0.95$, it used Duffie's assumptions about radiative sky temperatures, and it assumed typical values for heat loss through the back and sides of collectors. The comparisons all assume a constant flow rate of 10 cm^3/sec per square meter of collector area A_c and a fixed inlet temperature for collectors in Omaha. The "average" U-value used for the fixed U-value case was computed using the annual average daytime temperature and wind velocity.

It can be seen from table VII I-A-IO **that the total annual output agrees to within about 0.5 percent in all four cases run. The monthly totals vary by as much as 10** percent, but for the two-cover, selective absorber case which has thermal losses comparable to the tubular flat-plate collector generally modeled, the monthly differences are always less than 3 percent. During the winter, the fixed U-value approach gives less output than the variable U-value approach. This indicates that lower ambient temperatures during the winter decrease the U-value more than the increase due to higher wind velocities, even for single cover collectors.

The fixed U-value approach reduced the cost of computer computation by about 50 percent.